MOLECULAR DYNAMICS SIMULATIONS OF BUBBLE COLLAPSE AT SONOLUMINESCENCE CONDITIONS

Kurz, Thomas; Metten, Burkhard; Schanz, Daniel; Lauterborn, Werner
Drittes Physikalisches Institut, Universität Göttingen
Bürgerstrasse 42-44
37073 Göttingen
Germany
Tel.: +49(551) 39 7713
Fax.: +49(551) 39 7720
E-mail: Thomas.Kurz@dpi.physik.uni-goettingen.de

ABSTRACT
The physical processes within collapsing bubbles are investigated by molecular dynamics simulations with up to several million particles. The chosen bubble and driving parameters correspond to typical conditions of single-bubble sonoluminescence. Bubbles containing noble gas, noble gas mixtures and gas-vapor mixtures are considered. Mass and heat diffusion, heat conduction across the bubble wall, condensation of vapor at the gas-liquid interface, and dissociation reactions are taken into account. To demonstrate their effects typical examples of the evolution of temperature and density within the bubble are presented.

Introduction

The collapse of strongly excited bubbles in a liquid can generate very high central temperatures and pressures. The extreme conditions in the bubble trigger chemical reactions [1] and give rise to the phenomenon of sonoluminescence, i.e., the light emission of acoustically driven bubbles [1,2]. Sonoluminescence is long known as a faint glow of cavitating bubbles in insonicated liquids (MBSL – multi-bubble sonoluminescence) and has attracted considerable attention in the past decade after the discovery of single-bubble sonoluminescene (SBSL), the light emission of single, acoustically trapped cavitation bubbles [3].

Sonoluminescene light is composed of very short pulses that are emitted at the very moment of bubble collapse. Thus, they are very likely of thermal origin. Measurements of MBSL indicate maximum temperatures of about 5000-6000 K and optical spectra featuring emission bands. On the other hand, analysis of SBSL light gives smooth spectra without pronounced features that are compatible with blackbody or bremsstrahlung emission and temperatures in excess of 10000 K. These differences between SBSL and MBSL have been attributed, e.g., to perturbed collapse in multi-bubble systems (by bubble interactions) [1], but they could also be caused by an increase of collapse temperature, with corresponding change in light characteristics, when the driving pressure is increased. Furthermore, MBSL light is usually measured as an average over the emission of many bubbles that could have different and time-dependent emission properties. These unresolved issues motivate a thorough investigation of the collapse and the associated light emission of single bubbles under different conditions.

Apart from sonoluminescence, the characterization of physical conditions in highly compressed and heated bubbles and their dependence on parameters are of great interest for the understanding of bubble action, e.g. in cavitation damage and erosion, and for system opti-

mization in applications such as ultrasonic cleaning or sonochemistry. Currently, experiments do not permit to measure the spatiotemporal dynamics in a collapsed bubble, which is very small (~1 μm) and not resolvable by visible light. Sophisticated numerical simulations have to be used to study the physics taking place in the bubble [4,5] and to set up predictions that can be tested by experiment. In this endeavor, continuum fluid dynamics (CFD) models prevail. They work well in situations where the Knudsen number of the flow is small compared with unity.

In this work, a different numerical approach is taken: molecular dynamics (MD) simulation [6-9]. A typical SBSL bubble filled, e.g., with argon, has an equilibrium radius R_0 of the order of 4-10 μm, which implies that about 10^9 to 10^{10} atoms will occupy the bubble. For smaller bubbles the particle number now comes into reach of realistic MD simulations with present-day computers. As a first step, one to several million particles have been used in the scaled-down MD simulations of bubble collapse presented in this paper.

The MD method has several inherent advantages compared with CFD models. It naturally incorporates linear and nonlinear diffusion processes. It is three-dimensional and thus capable of capturing the spatiotemporal dynamics in complicated geometries down to very small scales, including the structure of shock fronts. MD is therefore not restricted to the spherically symmetric case as many simple bubble models are. The method can readily be extended without the necessity to augment the set of underlying model equations. On the other hand, the MD method is computationally demanding. It requires large amounts of computer memory and high CPU performance. To obtain a realistic simulation, the particle parameters (e.g., interaction cross sections) have to be known accurately. In the case of chemical reactions, all possible chemical reaction pathways have to be taken into account. Finally, ionization and the dynamics of charged particles (in particular, electrons) are notoriously difficult to simulate with MD because of the very small dynamical timescales and long-range interactions of the plasma constituents.

The Model

A bubble is modelled as a spherical container of varying radius $R(t)$ holding a large number N (about 10^6 or more) particles. These molecules are imagined as hard spheres that interact by elastic or inelastic collision upon direct contact; they have no long range interaction. A molecular species i is defined by the particle's mass m_i and diameter d_i. Molecules with rotational degrees of freedom are represented by spinning spheres which can also exchange angular momentum. The number of particles may change by mass transfer at the bubble wall (evaporation and condensation) and by dissociation and recombination in reactive collisions. All physical quantities are scaled to dimensionless form for the numerical calculations.

As is well known, the simulation of a hard-sphere gas can effectively be performed by an event-driven algorithm [6] because between collisions the particles propagate in rectilinear motion – gravity being neglected – and the time of the next collision can be calculated easily. The computer code keeps a calendar of all possible collisions (and further relevant events) and advances the time evolution from one event to the next.

The liquid is described as a continuous medium with a spherically symmetric flow field which is consistent with the assumed spherical shape of the bubble wall. The bubble's radial dynamics is calculated by an extended Rayleigh-Plesset equation that includes liquid viscosity and damping by acoustic radiation:

$$R\ddot{R} + \tfrac{3}{2}\dot{R}^2 = \frac{1}{\rho_L}(p_L - p_\infty) + \frac{R}{\rho_L c_L}(\dot{p}(R,t) - \dot{p}_\infty)$$

Here,

$$p_L = p(R,t) - \frac{2\sigma}{R} - 4\rho_L v \frac{\dot{R}}{R}$$

is the liquid pressure at the bubble wall, ρ_L the density of the liquid (here, water with ρ_L = 996.6 kg/m^3), c_L=1481 m/s the Eulerian speed of sound, v=8.569·10^{-7} m^2/s the kinematic viscosity, and σ=72.75·10^{-3} N/m the surface tension of the liquid. Note that in the calculations underlying Figs. 1-3 the surface tension was neglected. $p(R,t)$ is the pressure in the bubble at the wall and is

calculated by averaging over momentum transfer from wall collisions of the model particles. The liquid pressure far off the bubble,

$$p_\infty = p_0 + p_a(t) = p_0 - p_{d0} \sin \omega_d t$$

is composed of the static pressure p_0=1 atm and a sinusoidal acoustic driving pressure of amplitude p_{d0} = 1.3atm and frequency f_d=ω_d/2π=26.5 kHz. All of the forthcoming results were obtained for a bubble of rest radius R_0=4.5 μm and the above given numerical parameter values.

The rules of interaction of the model particles with the bubble wall define the mechanical and thermal boundary conditions. In our simulations, different implementations of these rules have been used: (i) in a reflective collision the particle's velocity component normal to the wall is reversed and increased by the amount of the wall velocity; (ii) a general thermal boundary condition is defined by adjusting the outgoing particle's temperature to T_r = (1-α_T)T_i + α_T T_W, where T_i is the temperature of the incident particle, T_W is the wall temperature and α_T is the thermal accomodation coefficient. With given T_W the case α_T =0 corresponds to adiabatic compression, and α_T =1 to isothermal compression. In the general case, a thermal boundary layer with quadratic temperature profile is assumed. It yields the wall temperature according to the heat power flowing through the bubble surface, calculated from particle impacts in a self-consistent way.

The macroscopic quantities (density, pressure, velocity, temperature) are obtained by averaging over a grid of cells of fixed volume (concentric shells) over a certain time interval. Therefore, the spatial resolution of averaged quantities decreases towards the bubble center. The MD simulation of a bubble collapse is started at maximum bubble expansion. As the initial condition, the particles are distributed on a regular grid in the volume with random velocities according to a Maxwellian distribution. It turns out that the initial regular arrangement is randomized after a few collision times. Note that as the initial bubble radius R_0 and density are prescribed the particle mass is fixed, and the molecules have to be interpreted as `quasiparticles' corresponding to a coarse-grained model of the real situation. Diffusion processes may thus be overestimated by our calculations.

Ionization is not yet implemented by particle collision. To calculate, e.g., the sonoluminescene light power, a simple Bremsstrahlung model is assumed, where the degree of ionization is derived from the temperature of the medium by means of the Saha equation. For more details on the implementation of the MD method, in particular, on the modelling of condensation and of chemical reactions, the reader is referred to Ref. 7 and a forthcoming publication [10].

Results

Heat conduction and particle diffusion and mixing in the gas are taken into account in an MD simulation by principle. To arrive at a realistic model of bubble collapse other relevant physical processes of bubble dynamics such as heat conduction across the wall, condensation of water vapor at the wall, and dissociation of vapor at high temperature, were successively incorporated in the model. In this way the influence of the various effects on the interior dynamics and their relative importance could be assessed.

Fig. 1 gives an example of the temperature distribution in a two-dimensional cross-section of a collapsing bubble composed of Argon gas with reflective boundary conditions and a total of 10^6 particles. An inward-traveling compression wave focuses at the center and yields a core temperature of about 10^5 K. Due to neglect of energy-consuming effects in this calculation (heat conduction into the liquid, condensation and dissociation) the maximum temperature is overestimated. The wave is reflected at the center and forms an outgoing compression wave heading towards the bubble wall (not shown).

Simulation runs have been performed with varying number of particles to assess the quality of the simulation in terms of convergence of the averaged solutions. The scaling analysis reveals that the number of particles in the simulation should be as large as possible to reduce errors. Insufficient particle numbers lead, for example, to the blurring of shock fronts. This makes the identification of shocks more difficult, as due to lack of discontinuities there is a gradual transition from compression to shock waves in the MD model.
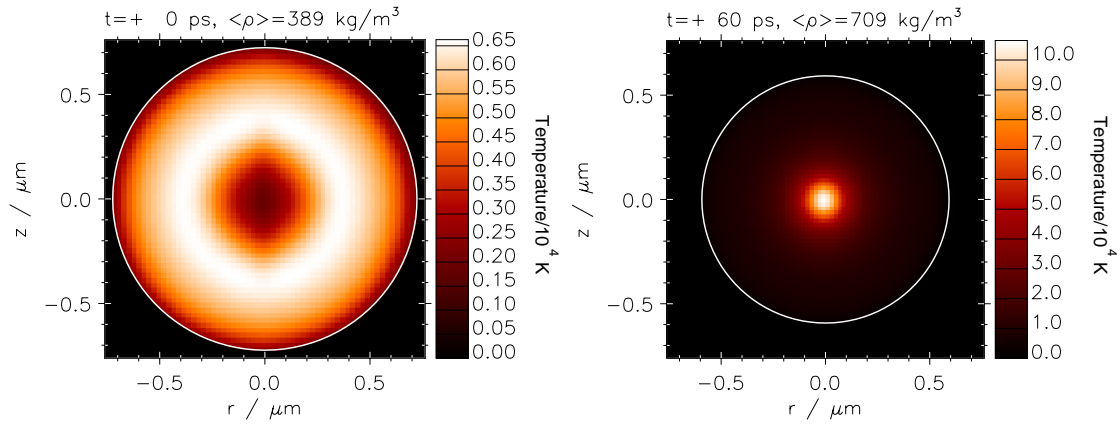
Fig. 1: Two-dimensional temperature distributions (100 x 100 cells) of a spherical Argon bubble with reflective boundary at start of compression (left) and at maximum compression (right).

In Fig. 2 temperature profiles are shown at different thermal boundary conditions for an Argon bubble with 10^6 particles. With adiabatic collapse (upper left) the central temperature reaches about 80000 K, and only relatively weak compression or shock waves are observed. In the isothermal case (upper right) the collapse is more violent, because the bubble takes up energy from the liquid while still expanding and thus reaches a larger maximum radius. The stronger collapse give rise to an ingoing shock wave; it is reflected at the center where a very high temperature (~200000 K) and density is attained. The case of a thermal boundary layer (lower left) with α_T=1 is similar to the isothermal case, but the collapse is less violent and slightly smaller core temperatures and densities are reached. Analysis of the conditions at the bubble wall reveals that heat inflow during bubble expansion is important for violent collapse and, thus, for the occurrence of extreme conditions in the bubble.
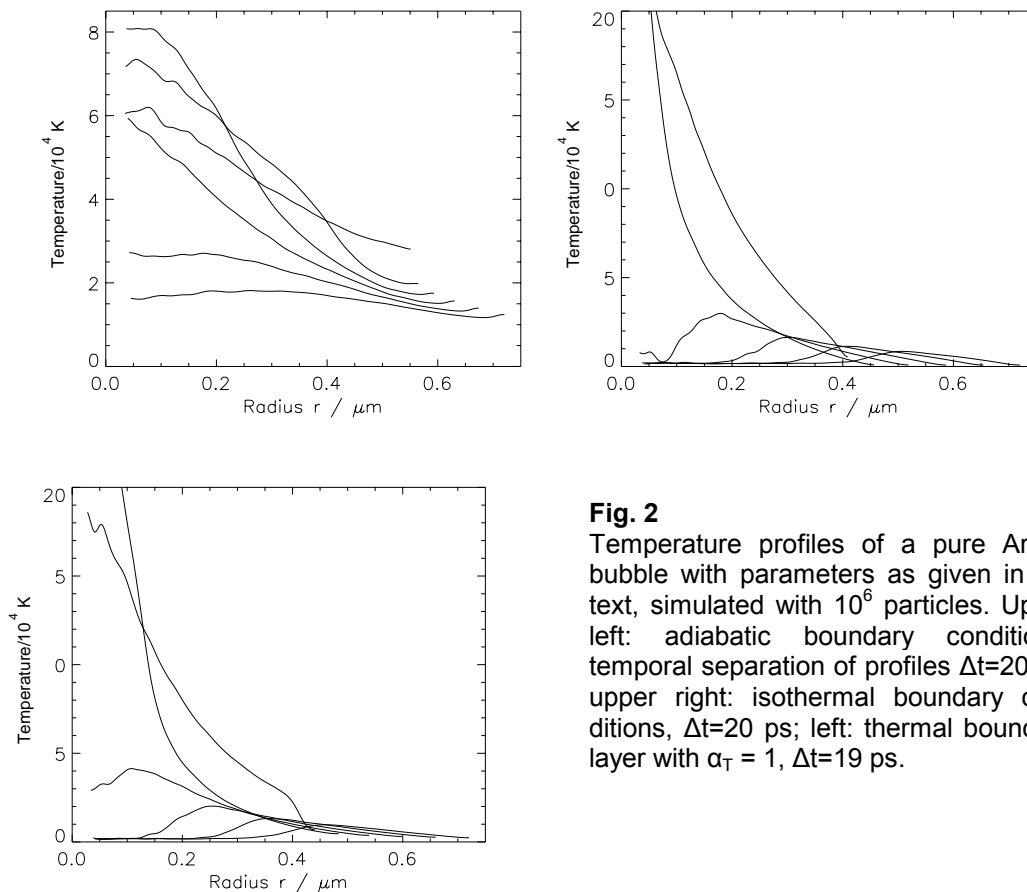

Fig. 2
Temperature profiles of a pure Argon bubble with parameters as given in the text, simulated with 10^6 particles. Upper left: adiabatic boundary conditions, temporal separation of profiles Δt=20 ps; upper right: isothermal boundary conditions, Δt=20 ps; left: thermal boundary layer with α_T = 1, Δt=19 ps.
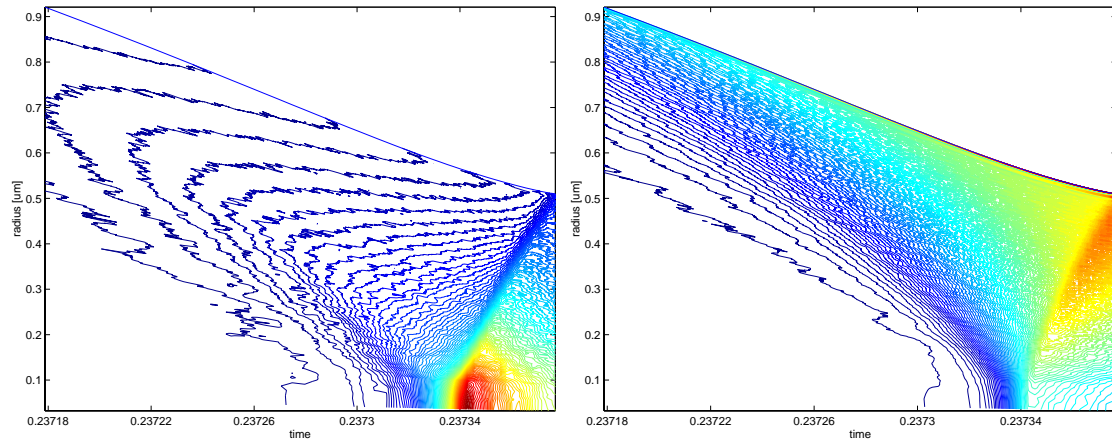
Fig. 3: Contours of temperature (left) and density evolution (right) of a spherical bubble containing Argon and water vapor. Condensation of vapor and heat transfer via a thermal boundary layer are taken into account (α_T=0.4).

In general, a bubble will contain several sorts of particles, for example, a mixture of noble gases in single-bubble sonoluminescence, or different species originating from sonochemical reactions (sonolysis). MD runs not detailed here reveal, as do CFD simulations [11], that species may be segregated in the bubble according to their molar mass. The process has a bearing on shock wave formation, chemical reactions in the bubble, transport of chemical species out of the bubble, and on sonoluminescence light characteristics.

Fig. 3 gives snapshots of the temperature and density field of an Argon bubble containing vapor. The thermal boundary layer, condensation and rotational degrees of freedom of the vapor particles are taken into account. This bubble reaches a larger maximum radius than the bubble without vapor, and therefore collapses more violently. The core temperatures are nevertheless similar to the previous case because the Argon accumulates at the center which leads to less heating. The outgoing shock is stronger than in the case without vapor.

These numerical results reveal that due to its accumulation at the bubble center and its non-equilibrium condensation a considerable amount of vapor is trapped in the bubble during the collapse. Vapor dissociation then becomes an important endothermal process that has been incorporated in further calculations. An example is presented in Fig. 4 (right) and compared to the case of a pure Argon bubble, and an Argon bubble with non-dissociating vapor (Fig. 4, left).
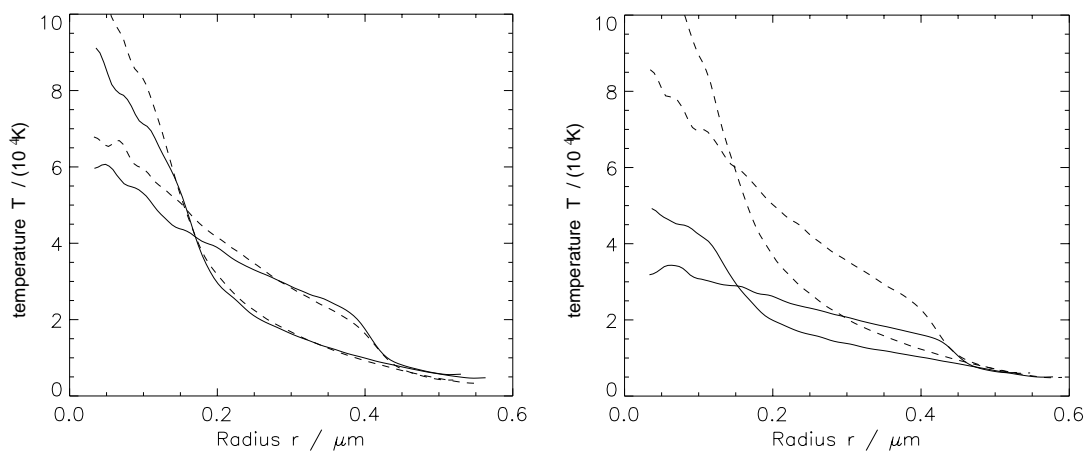

Fig. 4: *Left:* Temperature profiles of a spherical bubble containing Argon only (- - -) and containing a mixture of Argon and water vapor (—) at two moments around maximum compression; *right:* corresponding plot for an Argon-vapor bubble calculated with chemical reactions of 10 species (—) and without chemical reactions (- - -) .

With the water chemistry taken into account, the central temperature is lowered by about a factor of two in the later stages of collapse. This is qualitatively, not yet quantitatively, in accord with recent CFD calculations [12].

The sonoluminescene light emission computed from MD simulations of bubbles containing noble gas mixtures is given in Table 1. Light energies and pulse durations are at the lower end of, but compatible with the range of reported measurements of SBSL light [2,13]. The brighter sonoluminescemce of Xenon bubbles is predicted correctly.

gas mixture	Pulse duration [ps]	pulse energy [pJ]
He 100%	17.7	$1.2 \cdot 10^{-8}$
He 10% Ar 90%	39.7	0.28
He 1% Ar 99%	35.9	0.74
Ar 100 %	34.7	0.82
Ar 50% Xe 50%	80.3	1.0
Xe 100%	69.4	8.2

Table 1
Charactersitics of SBSL light from gas bubbles with thermal boundary layer ($\alpha_T=1$, $N=10^6$).

Conclusions
The molecular dynamics method is a versatile and powerful, yet computationally demanding tool to investigate the dynamics within small collapsing bubbles. With further improvement and extension, it can help to better understand the physics and chemistry within cavitating bubbles even in complex situations, e.g. with asymmetric collapse or bubble breakup, that prevail in applications such as ultrasonic processing or sonochemistry.

References
[1] L.A. Crum, ``Sonoluminescence, sonochemistry, and sonophysics´´, J. Acoust. Soc. Am. **95**, 559 (1994); K.S. Suslick, ``Sonochemistry: A physical perspective´´, in: W. Lauterborn, T. Kurz, (ed.), *Proc. 15th Int. Symp. on Nonlinear Acoustics*, Melville, New York: AIP, 2000, p. 95-104
[2] B.P. Barber, R.A. Hiller, R. Löfstedt, S.J. Putterman, ``Defining the unknowns of sonoluminescence´´, Phys. Rep. **281**, 65 (1997); D. Hammer, L. Frommhold, ``Topical review sonoluminescence: how bubbles glow´´, J. Mod. Optics **48**, 239 (2001)
 [3] D.F. Gaitan, L.A. Crum, ``Observation of sonoluminescence from a single, stable cavitation bubble in a water/glycerine mixture´´, in: M.F. Hamilton, D.T. Blackstock (ed.), *Proc. 12th Int. Symp. on Nonlinear Acoustics*, London: Elsevier, 1990, p. 459-463
[4] W.C. Moss, D.B. Clarke, D.A. Young, ``Calculated Pulse Widths and Spectra of a Single Sonoluminescing Bubble´´, Science **276**, 1398 (1997)
[5] K. Yasui, ``Temperature in multibubble sonoluminescence´´, J. Chem. Phys. **115**, 2893 (2001)
[6] D.C. Rapaport, *The Art of Molecular Dynamics Simulation*, Cambridge University Press, Cambridge, 1997
[7] B. Metten, *Molekulardynamik-Simulationen zur Sonolumineszenz*, Der Andere Verlag, Osnabrück, 2001 (in German)
[8] B. Metten, W. Lauterborn, ``Molecular Dynamics Approach to Single-Bubble Sonoluminesc-ence´´, in: W. Lauterborn, T. Kurz, (ed.), *Proc. 15th Int. Symp. On Nonlinear Acoustics*, Melville, New York: AIP, 2000, p. 429-432
[9] T. Kurz, W. Lauterborn, B. Metten, ``Molecular dynamics approach to bubble dynamics and sonoluminescence´´, Proc. 17th Int. Congr. on Acoustics (ICA17), Rome 2001, CD Vol. I
[10] T. Kurz, B. Metten, D. Schanz, W. Lauterborn, in preparation
[11] B.D. Storey, A.J. Szeri, ``Mixture segregation within sonoluminescence bubbles´´, J. Fluid Mech. **396**, 203 (1999)
[12] B.D. Storey, A.J. Szeri, ``Water vapour, sonoluminescence and sonochemistry´´, Proc. Royal Soc. London A **456**, 1685 (2000); R. Toegel, B. Gompf, R. Pecha, D. Lohse, ``Does water vapor prevent upscaling sonoluminescence?´´, Phys. Rev. Lett. **85**, 3165 (2000)
[13] B. Gompf, R. Günther, G. Nick, R. Pecha, W. Eisenmenger, ``Resolving sonoluminescence pulse width with time-correlated single-photon counting´´, Phys. Rev. Lett. **79**, 1405 (1997)